Structural Determinants in the Interaction of *Shaker* Inactivating Peptide and a Ca^{2+}-Activated K^+ Channel†

Ligia Toro,*,‡ Michela Ottolia,‡ Enrico Stefani,‡ and Ramón Latorre§

Department of Molecular Physiology and Biophysics, Baylor College of Medicine, Houston, Texas 77030, and Centro de Estudios Científicos de Santiago, Casilla 16443, and Department Biología, Facultad de Ciencias, Universidad de Chile, Santiago, Chile

Received February 16, 1994®

ABSTRACT: *Shaker* B inactivating peptide (BP) binds to its receptor in maxi K_{Ca} channels obstructing the flow of ions through them. The interaction between K_{Ca} channels and BP mutants, with different net charge and hydrophobicity, revealed several structural features of the K_{Ca} channel internal mouth. Increasing BP net positive charge or decreasing the internal milieu ionic strength increased the affinity and rate of association, while increasing hydrophobicity augmented blocking times and had limited or no effect on on-rates. These results uncover (a) the presence of negative charges in or near the BP receptor and (b) the existence of a hydrophobic contact surface in the internal channel vestibule that is a structural constituent of the BP receptor in maxi K_{Ca} channels.

The group of Aldrich (Hoshi et al., 1990; Zagotta et al., 1990) has identified the inactivation gate in *Shaker* B K^+ channel as the cytoplasmic domain of the channel-forming protein located in the amino terminus. Translated into the classical "ball-and-chain" model proposed by Armstrong and Bezanilla (1977) to explain Na^+ channel inactivation, the first 20 amino acid residues from the amino terminus conform the ball that hangs in the following 60 or so residues. One ball is able to swing into and to hinder ion flow by occluding the pore once this opens (MacKinnon et al., 1993); this gate behaves as an open-channel blocker (Choi et al., 1991; Demo & Yellen, 1991).

Differing from the *Shaker* channel, most K_{Ca} channels of large unitary conductance give rise to sustained macroscopic currents. This rule has a notable exception in the K_{Ca} channel from rat adrenal chromaffin cells that shows a fast inactivation process resembling that found in A-type K^+ channels (Solaro & Lingle, 1992). The inactivation process in the chromaffin cell channel can be removed by exposing the cytoplasmic side of the channel to trypsin. This result is consistent with the hypothesis that the "ball and chain" model may be applied to a family of K_{Ca} channels as well.

The synthesized *Shaker* B ball peptide (BP) is able to interact with non-inactivating K_{Ca} channels (Foster et al., 1992; Toro et al., 1992) and with trypsin-treated chromaffin K_{Ca} channels (Solaro & Lingle, 1992). K_{Ca} channel inhibition promoted by BP can be relieved competitively by internally added tetraethylammonium and by external K^+ (Toro et al., 1992). Therefore, in non-inactivating K_{Ca} channels the changes in channel gating kinetics induced by BP can be most simply interpreted in terms of a weakly voltage-dependent blockade that results from peptide binding to the internal mouth of the channel.

We have previously proposed that BP can be used to probe the internal vestibule of the K_{Ca} channel. Thus, the present work is an inquiry on the structural features of BP that regulate its binding to the K_{Ca} channel internal mouth. In this paper we show that increasing BP net charge increases peptide binding affinity by increasing exclusively the peptide association rate constant. We also show that mutations that made the BP more hydrophobic also induce a tighter peptide binding to the channel, but in this case the dissociation rate constant is the affected one. Moreover, on the basis of the results obtained with peptides with different net charges, we conclude that the voltage dependence of the blockade cannot be explained in terms of a charged blocking particle moving in the electric field to find its receptor. Finally, and consistent with the view that K_{Ca} channels possess a BP receptor similar to the receptor of *Shaker* B K^+ channels (Foster et al., 1992; Toro et al., 1992), equivalent structural features of the BP that define its interaction with K_{Ca} channels shown in this work have also been found to be required for the blockade of *Shaker* B K^+ channels (Murrell-Lagnado & Aldrich, 1993a,b).

NOMENCLATURE	SEQUENCE	NET CHARGE
WILD TYPE (BP)	MAAVAGLYGLGEDRQHRKKQ	2+
CHANGES IN: **CHARGED RESIDUES**		
K18QK19Q	MAAVAGLYGLGEDRQHRQQQ	0
R14Q	MAAVAGLYGLGEDQQHRKKQ	1+
R17Q	MAAVAGLYGLGEDRQHQKKQ	1+
K19Q	MAAVAGLYGLGEDRQHRKQQ	1+
E12ND13Q	MAAVAGLYGLGNQRQHRKKQ	4+
E12KD13K	MAAVAGLYGLGKKRQHRKKQ	6+
CHANGES IN: **HYDROPHOBIC RESIDUES**		
G6VG9V	MAAVAVLYVLGEDRQHRKKQ	2+
A2VA3VA5V	MVVVVGLYGLGEDRQHRKKQ	2+
CHANGES IN BOTH		
G6VG9VE12KD13K	MAAVAVLYVLGKKRQHRKKQ	6+
A2VA3VA5VE12KD13K	MVVVVLYVLGKKRQHRKKQ	6+

FIGURE 1: *Shaker* B inactivating peptide (ball peptide, BP) mutants. The primary sequence of BP and synthetic mutants is shown. Mutations are highlighted. The nomenclature of mutant peptides is given by original amino acid–position–new amino acid. This nomenclature is followed throughout the text and figure captions.

MATERIALS AND METHODS

Membrane vesicles from pig coronary artery were incorporated into lipid bilayers made of phosphatidylethanolamine: phosphatidylcholine:phosphatidylserine in a relation 5:3:2 at

† Supported by NIH Grant HL47382 (L.T.). R.L. was partially supported by Grants FNI 86391 and 1940227 and by institutional support to CECS (Santiago, Chile) provided by SAREC (Sweden) and a group of Chilean private companies (COPEC, CMPC, ENERSIS).

‡ Baylor College of Medicine.
§ Universidad de Chile.

® Abstract published in *Advance ACS Abstracts*, May 15, 1994.

0006-2960/94/0433-7220$04.50/0

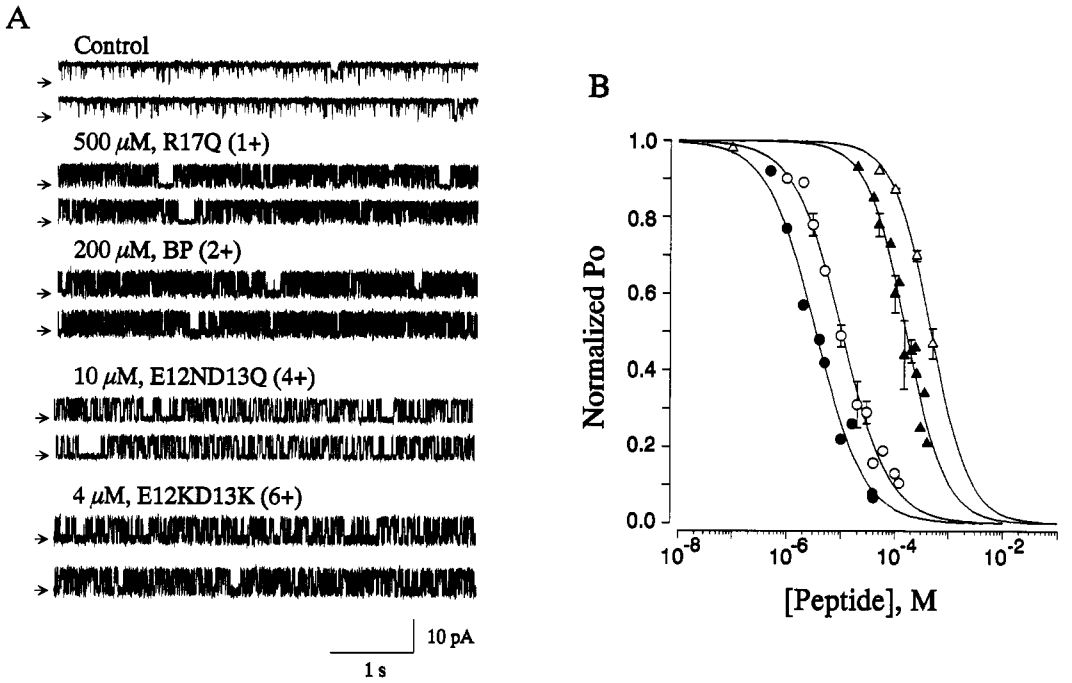

FIGURE 2: Mutant peptides with larger net charge are more effective blockers. (A) Examples of records obtained under control conditions, and upon addition of BP and mutants to the intracellular side of K_{Ca} channels from coronary smooth muscle, at concentrations near peptides' K_d's. Peptides' net charges are indicated in parentheses. P_o after peptide addition reached values near 0.5. As quantified in B, concentrations needed to obtain a half-maximal blockade of K_{Ca} channels diminished as net charge increased. (B) Dose–response curves fitted to eq 1 (see text). K_d values are as follows: R17Q (1+) (△), 474 ± 31 μM (n = 2); BP (2+) (▲), 160 ± 9 μM (n = 4); E12ND13Q (4+) (○), 10.7 ± 0.7 μM (n = 5); and E12KD13K (6+) (●), 3.6 ± 0.3 μM (n = 3). N values were near 1 (see Table 1). In this and the following figures, bars are SEM and holding potential is 0 mV.

Table 1: Blockade of a Maxi K_{Ca} Channel by Ball and Mutant Peptides

peptide	$K_d(0)^a$ (μM)	$K_d(0)^b$ (μM)	A^b	$N_{Hill}{}^a$	$k_{on}{}^c$ (s^{-1} M^{-1})
BP	160 ± 9	220 ± 14	0.44 ± 0.09	1.20 ± 0.10	(1.4 ± 0.3) × 10^6
K18QK19Q	259 ± 92	460 ± 170	0.39 ± 0.14	0.98 ± 0.10	(3.6 ± 0.71) × 10^5
R14Q	309 ± 59	623 ± 198	0.45 ± 0.04	1.09 ± 0.21	(6.9 ± 0.33) × 10^5
R17Q	474 ± 31	457 ± 123	0.43 ± 0.11	1.30 ± 0.13	(3.2 ± 0.60) × 10^5
K19Q	168 ± 5.5	152	0.37	0.95 ± 0.04	(1.1 ± 0.13) × 10^6
E12ND13Q	10.7 ± 0.7	11 ± 4.4	0.48 ± 0.08	1.00 ± 0.04	(7.3 ± 2.4) × 10^6
E12KD13K	3.6 ± 0.3	3.5	0.49	0.96 ± 0.08	(1.5 ± 0.07) × 10^7
G6VG9V	58.6 ± 8.7	125 ± 3.5	0.42 ± 0.2	0.87 ± 0.12	(9.3 ± 2.5) × 10^5
A2VA3VA5V	5.5 ± 1.1	6.6 ± 2.4	0.37 ± 0.07	0.79 ± 0.16	(1.6 ± 0.18) × 10^6
G6VG9VE12KD13K	1.10 ± 0.1	0.9 ± 0.3	0.46 ± 0.04	1.01 ± 0.14	(4.4 ± 0.9) × 10^6
A2VA3VA5VE12KD13K	0.166 ± 0.04	0.121 ± 0.011	0.5 ± 0.1	1.4 ± 0.39	(4.2 ± 0.53) × 10^6

[a] Values calculated from a Hill plot from experiments done at 0 mV. [b] Values obtained from a fit to the data using eq 8 (see text). [c] k_{on} was obtained from the slope of a plot of $1/\tau_0$ vs [peptide], except for A2VA3VA5V, G6VG9VE12KD13K, and A2VA3VA5VE12KD13K peptides, where $1/\tau_{burst}$ was used due to their slow blockade; experiments were carried out at 0 mV. The number of experiments varied from one to seven. For peptide abbreviations, see Figure 1. Values are means ± SD. Mean values for all peptides are A = 0.44 ± 0.043, N = 1.05 ± 0.17.

25 mg/mL, as previously described (Toro et al., 1991). The vesicles were applied to the preformed bilayer from the *cis* side, which was the voltage-controlled side, while the *trans* side was referred to ground. The internal side of the channel was determined by its voltage sensitivity. Continuous recording of channel activity was done using, in the *cis* side, a solution composed of (mM) 250 KCl, 5 MOPS-K, 0.1 $CaCl_2$, pH 7.4 and, in the *trans* side (mM), 250 NaCl, 5 MOPS-K, 0.1 $CaCl_2$, pH 7.4. Only channels whose internal side was facing the 250 mM KCl solution were used in this study. Recordings were filtered at 0.5–1 kHz using an eight-pole Bessel filter and acquired at 400–1000 μs/point. Single-channel analysis was performed using TRANSIT (A. M. J. Van Dongen, Department of Pharmacology, Duke University). Burst analysis was performed using IPROC (Axon Instruments, Burlingame, CA). Open probability (P_o) was obtained from the ratio between the open time and the total time. All analyses were performed in bilayers with a single channel. Unless otherwise stated, data are expressed as means ± SD. Peptides were synthesized and purified by HPLC in the Analytical Chemistry Center at the University of Texas, Health Science Center, at Houston.

RESULTS

Increasing Peptide Net Charge Increases Peptide Affinity. Figure 1 shows the structure of the *Shaker* inactivating peptide (BP) and the different point or double mutations made to modify the peptide net charge. At a working pH of 7.4 the various peptides have net charges ranging from 0 for the K18QK19Q peptide to +6 for the E12KD13K peptide. Considering that the pK_a for histidine in a protein is 6.5–7 (Cantor & Schimel, 1980), at pH 7.4 histidine 16 contributes little to the peptide net charge. We investigated the interaction of each of these peptides with single Ca^{2+}-activated K^+ channels in order to study the effect of the different structural modifications on the blocking kinetics.

Figure 2A shows examples of single Ca^{2+}-activated K^+ channel records obtained in the presence of peptides having

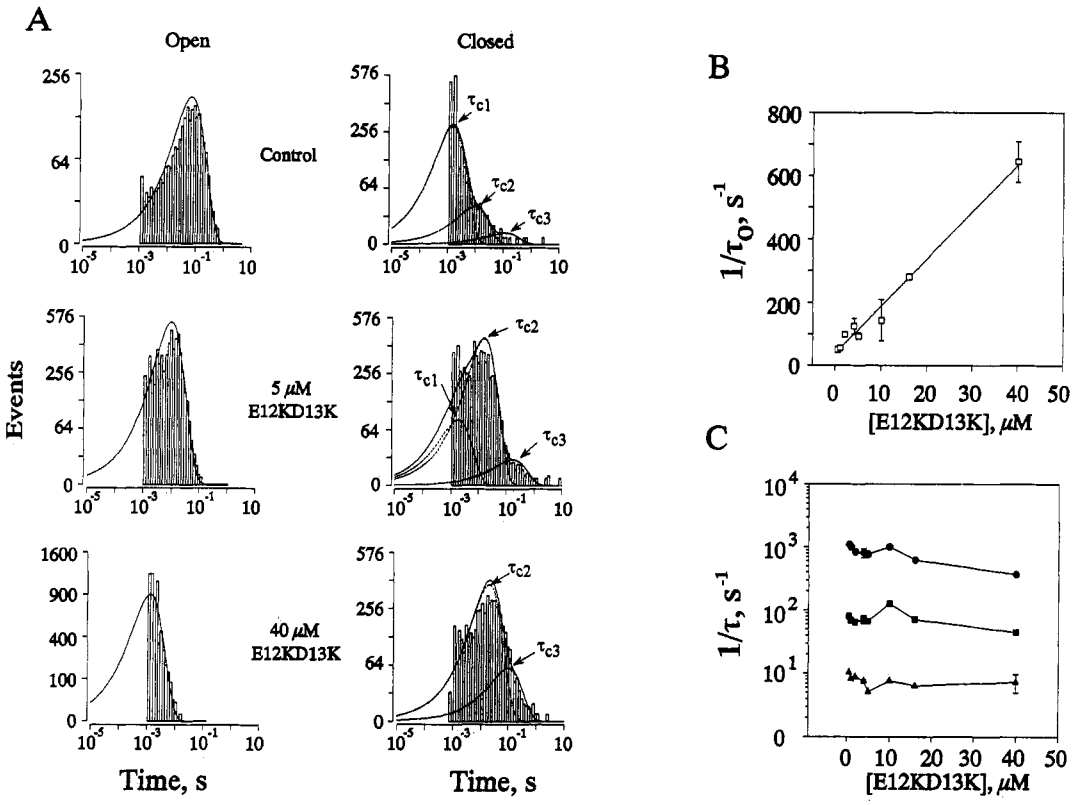

FIGURE 3: Open time varies proportionally to peptide concentration in peptides with polar mutations. (A) Open and closed time histograms of a K_{Ca} channel in control and after addition of a highly charged peptide mutant, E12KD13K (+6). Peptide addition caused a decrease in open times and the appearance of blocked events (with time constants similar to those present in control conditions). Open times were fitted to a single exponential; peak values correspond to the open time constant (τ_o), which diminishes as a function of [E12KD13K]. τ_o is 75 ms (control), 10 ms (5 μM peptide), and 1.4 ms (40 μM peptide). The number of events was 2271, 5908, and 5090, respectively. Values of closed time constants (τ_c) did not change significantly by increasing [peptide]; instead, increasing [peptide] augmented the number of events in each blocked state (τ_{c2} and τ_{c3}) and diminished the number of events of the normal closed state of the channel (τ_{c1}). Under control conditions time constants similar to those of the blocked times were present. τ_{c1} was 1.6 ms (90%) (control) and 1.3 ms (26%) (5 μM peptide). At 40 μM peptide, events of this duration were too few and a time constant could not be fitted. τ_{c2} was 12 ms (9%), 16 ms (72%), and 21 ms (87%), and τ_{c3} was 120 ms (1%), 195 ms (2%), and 111 ms (13%), in control, 5 μM peptide, and 40 μM peptide, respectively. (B) $1/\tau_o$ *vs* [E12KD13K] curve. k_{on} was 1.5×10^7 s^{-1} M^{-1}. (C) $1/\tau_c$ *vs* [E12KD13K] curve: τ_{c1} (●), τ_{c2} (■), τ_{c3} (▲). Number of channels = 3. Percentage values in parentheses in this figure and in Figure 6 indicate the percent of the total number of events that contributed to that particular kinetic component.

a smaller (e.g., R17Q) or a larger (e.g., E12KD13K) net charge than the wild type BP. The control record shows brief closing events, and the calculated probability of opening is 0.94. Addition of the peptides to the cytoplasmic side of the channel induces the appearance of an excess of fast fluctuations, which have been interpreted for the case of the BP as blocking events (Toro et al., 1992), and causes a reduction in P_o. Figure 2A illustrates that the concentrations of peptide needed in order to decrease P_o to ≈0.5 become smaller as the net positive charge of the peptide is increased. This is a clear indication that increasing peptide positive net charge promotes an increase in the peptide affinity for the channel. The effect of the change in net charge of the different peptides tested is quantified in Figure 2B, where the normalized P_o is plotted as a function of peptide concentration (for a summary of results, see Table 1). In all cases the data are well described by the relation

$$\text{normalized } P_o = K_d/([P]^N + K_d) \qquad (1)$$

where [P] is the peptide concentration, K_d is the dissociation constant for the peptide binding reaction, and N is the Hill coefficient. Note that the average value for N, 1.05, implies that a single peptide molecule is sufficient to fully block the channel (Table 1). However, the affinities for the different charged mutants are vastly different. In fact, Figure 2B and Table 1 demonstrate that the peptide E12KD13K (+6) binds to the channel about 132-fold more tightly than R17Q (+1).

The blockade induced by the different peptides (Figure 1 and Table 1) shared the following characteristics: (a) blockade is relieved by increasing the *external* K^+ concentration; and (b) regardless of their binding strength, all peptides are active only when added to the internal side of the channel. Therefore, for the coronary Ca^{2+}-activated K^+ channel the changes in channel kinetics induced by the different peptides tested can be most simply interpreted in terms of a peptide binding to the internal mouth, and hindering ion flow through the channel.

Only the Second-Order Rate Constant Is Modified by Changes in Peptide Net Charge. From records as those shown in Figure 2A we have extracted the distribution of open and closed dwell times as a function of peptide concentration. We found that, for all the peptides in Table 1, the dwell times in the open state are distributed as a single exponential, but the distribution of closed dwell times is clearly multiexponential. As a typical case, in Figure 3A we show the dwell time histograms for the case of the E12KD13K peptide. Note that, for the three concentrations tested, mean open times became shorter as the concentration of peptide was increased. On the other hand, as found for BP (Toro et al., 1992), addition of this peptide to the cytoplasmic side of the channel modifies mainly the number of events in the different closed states without modifying in an appreciable manner their time constants. Figure 3B shows that the mean open time varies

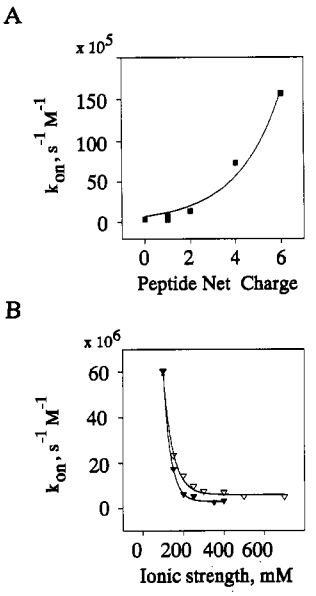

FIGURE 4: Association rate constant varies with peptide net charge and ionic strength. (A) k_{on} *vs* peptide net charge. k_{on} values for K18QK19Q (0), R14Q (1+), R17Q (1+), K19Q (1+), E12ND13Q (4+), and E12KD13K (6+) were graphed (see Table 1). Values were fitted to eq 3, giving −13 mV for the electrostatic potential (ϕ) at the receptor site. (B) k_{on} *vs* ionic strength curve. Values at different KCl (▽) concentrations are means of two experiments. Similar k_{on} values were obtained in NaCl (▼). In contrast, k_{off} values did not vary significantly (not shown).

inversely with [E12KD13K]. If the blocking reaction proceeds according to the scheme

$$C \underset{\alpha}{\overset{\beta}{\rightleftharpoons}} O \underset{k_{off}}{\overset{k_{on}[P]}{\rightleftharpoons}} OP_1 \underset{k_{-1}}{\overset{k_1}{\rightleftharpoons}} OP_2 \ldots \qquad \text{(R-1)}$$

where C and O are the open and closed states, respectively, and OP_i's are blocked states, the slope of the straight line shown in Figure 3B gives the association rate constant (k_{on}) for peptide binding to the channel, inasmuch as the mean open time (τ_o) for a flickering blockade is given by the relation

$$1/\tau_o = \alpha + k_{on}[P] \qquad (2)$$

For the E12KD13K peptide, $k_{on} = 1.5 \times 10^7\ M^{-1}\ s^{-1}$. Figure 3C shows that the closed times are peptide concentration independent, which is also a prediction of reaction scheme R-1. Kinetic schemes able to account for the properties of BP blockade of the K_{Ca} channel will be analyzed in the Discussion.

The association rate constants for the peptides containing different net charges are shown in Table 1 and Figure 4A. The results strongly suggest that the whole effect of varying net charge on the equilibrium peptide binding can be explained on the basis of an increase in k_{on}. k_{on} increases as the *positive* peptide net charge is increased. An increase in k_{on} as the apparent net charge is increased suggests that the bimolecular association rate constant of peptide is influenced by the fixed negative surface charge in or in the neighborhood of the peptide receptor. This is not surprising since Villarroel (1989), using ion permeation and blockade strategies, determined that the internal mouth of a skeletal muscle K_{Ca} channel should have a surface charge density of 0.016–0.3 $-e/nm^{-2}$. This situation would predict that the local concentration of positvely charged peptides near the receptor would be higher than the concentration of neutral peptides. As pointed out by Moczydlowski et al. (1986), the observed zero-voltage second-order rate constant k_{on} would be expected to vary as a Boltzmann distribution with respect to the net charge, z, and the electrostatic potential at the receptor site, ϕ, as follows:

$$k_{on}(z) = k_{on,\phi=0} \exp(-zF\phi/RT) \qquad (3)$$

where $k_{on,\phi=0}$ is the rate constant in the absence of any surface potential. The solid line in Figure 4A is a fit to the data using eq 3 with $\phi = -13$ mV at an ionic strength of 250 mM. The above calculations are only qualitative in nature since the charged peptides considered here are not point charges. For example, the minimum distance between the charge located at K19 and E12 is ≈2.8 nm, which is about 3.5-fold the Debye length in the 0.25 M monovalent solution used in these experiments. In other words, it is expected that the peptides, due to their large size, exert a smaller effect on the potential than that predicted by the classic screening theory [*e.g.*, Alvarez et al. (1983)]. According to the above results, the binding of the charged peptides to the K_{Ca} channel should be sensitive to ionic strength. As shown in Figure 4B, the second-order rate constant for the E12KD13K peptide is high at low ionic strength and falls precipitously in the ionic strength range between 100 and 300 mM, and at larger ionic strength remained rather constant. Over the same range, the slowest mean closed time decreases only about 2-fold. The lowering of the on-rate constant by increasing ionic strength is understandable as an effect of local electrostatic fields near the channel's internal mouth [*e.g.*, MacKinnon and Miller (1988)]. Furthermore, consistent with the involvement of nonspecific electrostatic contributions to the binding of the peptide to the K_{Ca} channel, the on-rate is reduced in a similar manner by Na^+ (Figure 4B). Note that the on-rate constant at 700 mM KCl is $4.6 \times 10^6\ M^{-1}\ s^{-1}$, a value several orders of magnitude lower than the one expected for a diffusion-controlled rate.

Peptide Hydrophobicity and Peptide Binding. It is clear from Figure 1 that the BP contains two clearly distinct domains: in amino acid residues 1–10 there is a prevalence of hydrophobic amino acids, whereas residues 11–20 are either charged or polar in nature. We have changed the BP hydrophobicity by replacing alanines in positions 2, 3, and 5 by valines (A2VA3VA5V) and also by replacing glycines in positions 6 and 9 by valines (G6VG9V). Figure 5A shows single-channel current records obtained in the absence (control) and in the presence of these two "hydrophobic" analogues of BP. It is clear that, by making the peptide more hydrophobic, not only do they bind more tightly to the internal mouth of the channel but also the current record structure is different from that obtained with the charged analogues. This is clearly so when one compares, for example, the mutants E12KD13K and A2VA3VA5V; both peptides bind with the same strength ($K_d \approx 4\ \mu M$); however, the quiescent periods for the hydrophobic peptide are much longer than for E12KD13K. It appears then that making the peptide more hydrophobic increases the residence time of the blocking molecule in the receptor site. The peptide "glues" better to the internal mouth.

Figure 5B shows the normalized P_o *vs* [peptide] curves for G6VG9V and A2VA3VA5V. The data are well described by eq 1 with a Hill coefficient of ≈1 and dissociation constants of 58.6 and 5.5 μM, respectively. The results presented here suggest that one of the major energy factors favoring the partitioning of the BP and analogues from the aqueous solution into the receptor located in the channel-forming protein are hydrophobic interactions. The differences in transfer energies ($\Delta\Delta G_T$) between BP and the hydrophobic mutants can be

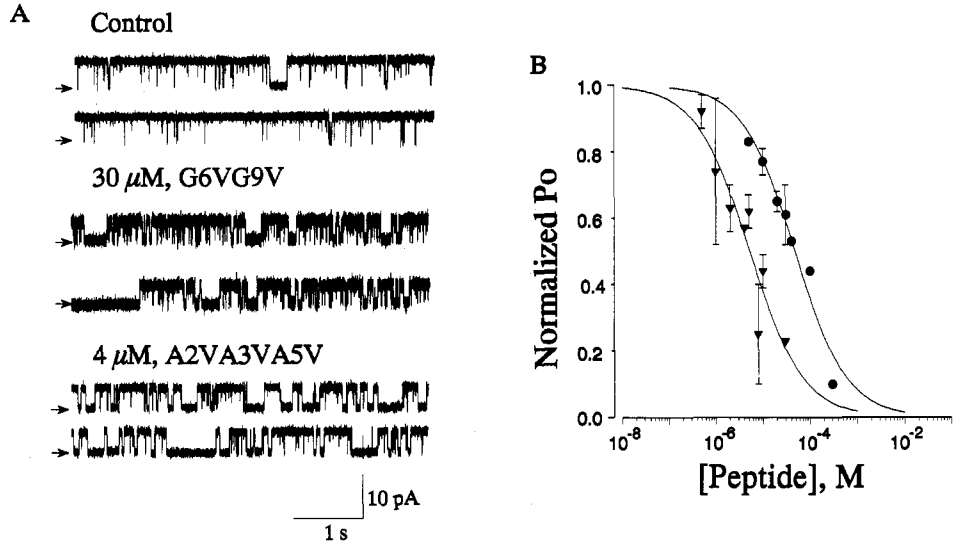

FIGURE 5: Increasing hydrophobicity increases peptide binding. (A) Channel records showing typical channel activity before and after addition of hydrophobic BP mutants. Note that increasing hydrophobicity not only increases peptide affinity (B) but also increases the duration of the blocked times. In mutant G6VG9V fast blocking events prevail; in contrast, in mutant A2VA3VA5V slower blocking times predominate. $P_o > 0.9$ in control and $P_o \approx 0.5$ after 30 μM G6VG9V or 4 μM A2VA3VA5V. (B) Normalized P_o vs [peptide] curves. Values were fitted to eq 1 (see text). K_d values are as follows: G6VG9V (●), 58.6 ± 8.7 ($n = 6$); and A2VA3VA5V (▼), 5.5 ± 1.1 ($n = 5$). N was near 1 (Table 1).

estimated from the ratio, K_d^{BP}/K_d^{mutant}, of the equilibrium dissociation constant of BP to that of a particular mutant by

$$\Delta\Delta G_T = -RT \ln(K_d^{BP}/K_d^{mutant}) \quad (4)$$

$\Delta\Delta G_T$ is −0.59 kcal/mol when the ratio K_d^{BP}/K_d^{G6VG9V} is considered and −1.99 kcal/mol for the ratio $K_d^{BP}/K_d^{A2VA3VA5V}$.

Hydrophobicity Affects the Peptide Residence Times in the Internal Mouth. When the residence time of the molecule in the site is very long, channel kinetics can be described as having periods in which the channel is active (a burst), interrupted by long periods of quiescence. It is clear that the A2VA3VA5V peptide shows this type of kinetics. In this case k_{on} is related to the mean burst time (τ_{burst}) according to the equation

$$1/\tau_{burst} = k_{on}[P]/(1 + \alpha/\beta) \quad (5)$$

We have analyzed the blocking kinetics induced by A2VA3VA5V, and Figure 6A shows the dwell time histograms for the open and closed dwell times. Differing from the charged mutant peptides described in previous sections, increasing the concentration of A2VA3VA5V peptide does not greatly modify the mean open time. On the other hand, this peptide induces the appearance of two closed states that were not present in the control, indicated as τ_{c3} and τ_{c4} in Figure 6A. These two time constants are independent of peptide concentration, but addition of A2VA3VA5V induced a reduction in the number of short events ($\tau_{c1} \approx 1.5$ ms) and a marked increase in the number of events comprising the population characterized by $\tau_{c3} \approx 100$ ms. For example, addition of 4 μM A2VA3VA5V causes a decrease in the number of events of the τ_{c1} kinetic component from 83% to 54%, and an increase in [P] from 0.5 μM to 4 μM increases the number of events of the τ_{c3} component from 5% to 15%. Figure 6B shows that for this particular peptide $1/\tau_{burst}$ is directly proportional to [A2VA3VA5V]. The slope of the curve gives a k_{on} of 1.6×10^6 M^{-1} s^{-1}, which is very similar to that obtained for the wild type ball peptide (see Table 1) and about 10-fold smaller than that obtained for E13KD13K, a peptide with a similar dissociation constant. These results strongly suggest that increasing peptide hydrophobicity affects mainly the time the peptide resides in the internal mouth and not the frequency at which it hits successfully the receptor. Note also that despite the fact that the A2VA3VA5V peptide binds 10-fold better than G6VG9V (in this case $1/\tau_{on}$ is directly proportional to [G6VG9V]), their association rate constants with the receptor are not very different, strengthening the argument that changes in hydrophobicity of the peptide affect the rate of peptide dissociation.

Effects of Changing Peptide Net Charge and Hydrophobicity Are Additive. Figure 7A shows that the G6VG9VE12KD13K peptide induces a slow blockade typical of the hydrophobic mutants, but the blockade kinetics does not resemble that induced by the parent peptides G6VG9V (Figure 5A) and E12KD13K (Figure 2A). G6VG9VE12KD13K shows a much slower kinetics than the parent peptides; and its K_d is about 145-fold smaller than that of BP (Figure 7B), giving a $\Delta\Delta G_T$ of −2.95 kcal/mol. If the effects of changing peptide hydrophobicity and net charge are additive, we should have

$$\Delta\Delta G_T = -RT[\ln(K_d^{BP}/K_d^{G6VG9V}) + \ln(K_d^{BP}/K_d^{E12KD13K})] \quad (6)$$

Using the values for the K_d's shown in Table 1 and eq 6, we obtain a $\Delta\Delta G_T$ of −2.84 kcal/mol, a value which is close indeed to the value obtained experimentally. For A2VA3VA5VE12KD13K peptide $\Delta\Delta G_T$ = −4.07 kcal/mol, whereas the additivity condition of net charge and hydrophobicity effects predicts a $\Delta\Delta G_T$ of −4.24 kcal/mol; the similarity in values shows again that the effects of peptide charge and hydrophobicity in determining binding strength are additive.

The k_{on} expected for these peptides should be that of E12KD13K. We found that, as expected from a slow blockade, the mean open time is independent of peptide concentration, but $1/\tau_{burst}$ is directly proportional to [G6VG9VE12KD13K] (Figure 7C). k_{on} obtained from the slope of the straight line is 4.4×10^6 M^{-1} s^{-1}, which is in reasonable agreement with the k_{on} of E12KD13K, suggesting again that changes in peptide charge and hydrophobicity contributed independently to

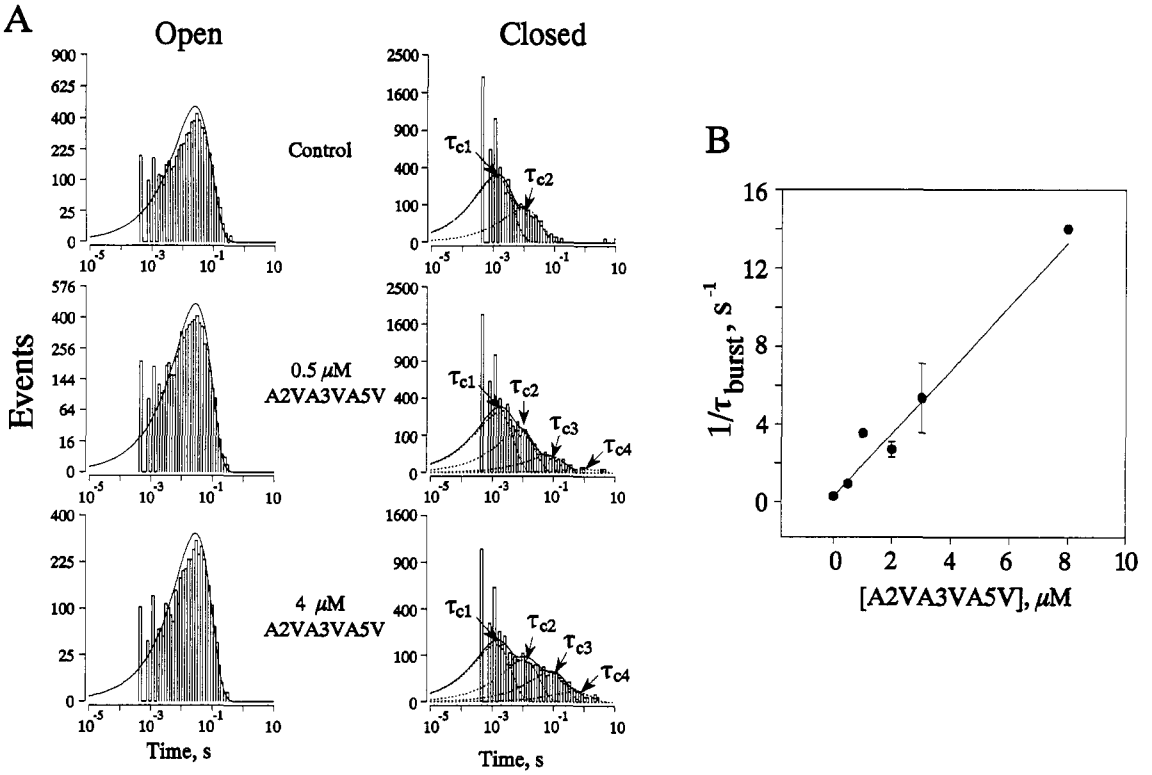

FIGURE 6: Burst time varies proportionally to peptide concentration in slow blocking hydrophobic mutants. (A) Open and closed time histograms of a K_{Ca} channel before (control) and after addition of 0.5 and 4 μM A2VA3VA5V mutant peptide to the internal side of the channel. Peptide addition produced slow blocked events (τ_{c3} and τ_{c4}) and practically no change in the open times (τ_o). τ_o were 29 ms (control), 26 ms (0.5 μM peptide), and 31 ms (4 μM peptide). The number of events was 5885, 6199, and 3998, respectively. Blocked times were independent of [peptide], but their number increased by augmenting [peptide]. Values were, for τ_{c3}, 73 ms (5%) and 87 ms (15%); and for τ_{c4}, values were 1 s (0.2%) and 0.5 s (2%) after 0.5 and 4 μM peptide, respectively. Note that the value of τ_{c4} at 0.5 μM peptide is not accurate since at this [peptide] there were few blocked events. Values for the channel intrinsic closed times (τ_{c1} and τ_{c2}) were, for τ_{c1}, 0.8 ms (83%), 1.5 ms (63.8%), and 1.3 ms (54%), and for τ_{c2}, 9.8 ms (17%), 8.1 ms (31%), and 11.3 ms (29%), before (control) and after 0.5 and 4 μM peptide, respectively. (B) $1/\tau_{burst}$ *vs* [A2VA3VA5V] curve. k_{on} was 1.6×10^6 s^{-1} M^{-1}. Number of channels = 5.

peptide binding characteristics. Accordingly, k_{on} for A2VA3VA5VE12KD13K is 4.2×10^6 M^{-1} s^{-1} (Table 1).

Voltage Dependence of the Blockade. All the peptides listed in Table 1 exhibited voltage dependent equilibrium constants, and the effect of voltage on peptide binding is given by the A parameter. We have previously shown for BP that its equilibrium binding is enhanced as the applied voltage becomes more positive (Toro et al., 1992). For BP we assumed that K_d is well described by the relation

$$K_d(V) = K_d(0) \exp(-AV) \quad (7)$$

where $K_d(0)$ is the zero-voltage dissociation constant and A is a constant which contains the voltage dependence of the blockade reaction. Combining eqs 1 and 7, we have

$$P_o = \{1 + [P]/K_d(0) \exp(-AV)\}^{-1} \quad (8)$$

The data for all different charged peptides were fitted according to eq 8. These results are summarized in Table 1. An unambiguous result of the present experiments is that the voltage dependence (A) of peptide binding is not related to the net charge of the peptide. A satisfying result is the good agreement found between the K_d's calculated using eq 1 (Table 1) and those obtained by means of eq 8.

DISCUSSION

In the present work we have shown that BP mutants are able to interact with K_{Ca} channels only from the cytoplasmic side, and because the inhibition of channel activity was relieved by external K^+, we located the interaction site in the internal mouth of the channel [Toro et al., 1992; see also Foster et al. (1992)]. We found that long-range electrostatic *and* hydrophobic interactions are crucial in determining the binding strength of a given peptide to the internal mouth of coronary K_{Ca} channels. These are the same structural determinants that modulate peptide binding to *Shaker* B K^+ channels (Murrell-Lagnado & Aldrich, 1993a,b).

The free energy differences expected from the change in hydrophobicity promoted by changing glycines to valines in the case of the G6VG9V peptide, or alanines to valines in the case of the A2VA3VA5V peptide, is −3 kcal/mol. This value is obtained by taking relative hydrophobicities of 0.5 and 1.5 kcal/mol for alanine and valine, respectively (Nozaki & Tanford, 1971; Tanford, 1980). These values represent the additional free energy of transfer from water to an organic solvent that is generated when the side chain of a given amino acid is substituted for the hydrogen atom of a glycyl residue; *i.e.*, the relative hydrophobicity of glycine in this scale is 0. How can we rationalize that, despite the fact that the two hydrophobic mutants we constructed have the same relative hydrophobicities when compared with the wild type peptide, the A2VA3VA5V binds 10-fold better to the channel internal mouth than the G6VG9V peptide? Note, first, that the value of $\Delta\Delta G_T$ obtained from the ratio $K_d^{BP}/K_d^{A2VA3VA5V}$ is much closer (−1.99 kcal/mol) than that obtained from the ratio K_d^{BP}/K_d^{G6VG9V} (−0.59 kcal/mol) to the expected ΔG_T of −3 kcal/mol and, second, that the alanines we replaced by valines are closer to the N-terminus than glycines 6 and 9. We suggest that the difference between these two hydrophobic BP analogues arises as a consequence of the position of the mutated

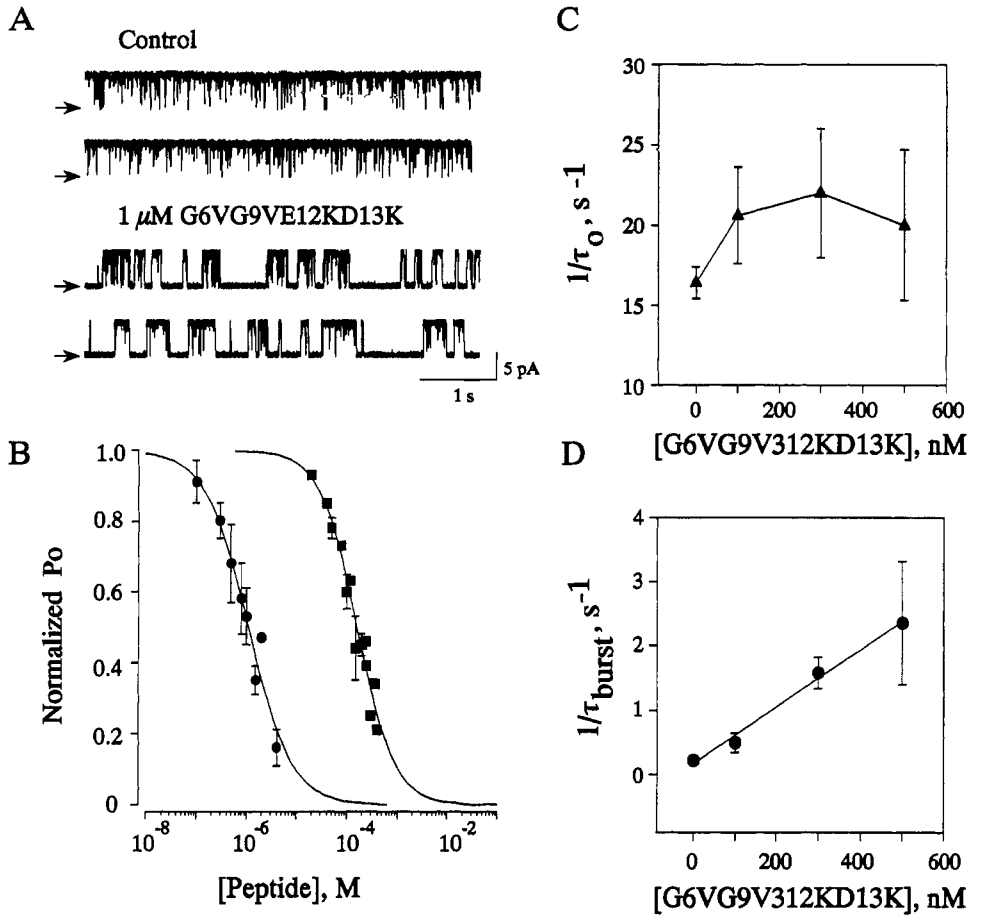

FIGURE 7: Blocking properties of a double type mutant with increased hydrophobicity and polarity. (A) Records of channel activity before and after addition of 1 μM G6VG9VE121KD13K to the internal side of the channel. Note the long blocked times and the absence of fast blocked states typical of the parent peptides E12KD13K (see Figure 2) and G6VG9V (see Figure 5). (B) Dose–response curves for G6VG9VE12KD13K (●) and BP (■). K_d was 1.1 ± 0.1 μM for G6VG9VE12KD13K (n = 7) and 160 ± 9 μM for BP (n = 4). N values were near 1 (see Table 1). (C) $1/\tau_o$ *vs* [peptide] plot. The open time constant was independent of peptide concentration as expected for a slow type of blockade. (D) $1/\tau_{burst}$ *vs* [peptide] plot. k_{on} was 4.4 × 10^6 M^{-1} s^{-1}. In C and D, number of channels = 7.

amino acids. The fact that increasing hydrophobicity increases the stability of peptide binding to the receptor speaks in favor of the presence of a hydrophobic "pocket" in the channel internal mouth. We propose that this pocket can accommodate amino acid residues 1–8 from the N-terminus. Hence, valine in position 6 of the mutant peptide would be the only residue that contributes to the hydrophobic effect in G6VG9V and, therefore, the expected ΔG_T would be only 1.5 kcal/mol. In other words, valine in position 9 "falls" out of the pocket. The "pocket" can be envisioned as a surface in the protein which makes contact with the interaction surface of the BP in the bound peptide–channel complex. In other words, for structural reasons, glycine 9 cannot be buried in the hydrophobic region that forms part of the peptide–channel contact surface. However, the experimental value of −0.59 kcal/mol obtained for the G6VG9V mutant is about half of the expected value for the transfer energy of the side chain of the valine 6 residue. Therefore, the low value for the transfer energy for the mutant peptide can be due to a partial "solvation" of the lateral valine 6 chain by the hydrophobic surface of the channel in the bound peptide–channel complex. We are confident that the hydrophobic region present in the internal mouth can also accommodate leucine 7 since replacement of this residue by glutamate dramatically decreases peptide binding in K_{Ca} channels, in *Shaker* B K^+ channel, and in a K^+ channel from epithelial cells as well (Zagotta et al., 1990; Dubinsky et al., 1992; Foster et al., 1992; Toro et al., 1992). Consistent with this view, recent studies in *Shaker* B K^+ channels demonstrated that increasing hydrophobicity at position 7 made the binding of the mutant "ball" peptides tighter (Murrell-Lagnado & Aldrich, 1993a).

Our kinetic studies indicated the presence of several blocked states (Toro et al., 1992). This has been corroborated in the present study for all the peptides tested. Notice, for example, the presence of at least three blocked states in Figure 6. It is difficult at present to ascribe a molecular origin to the different blocked states. However, they may arise as a consequence of either the presence of several different structural forms of the peptide in solution that bind to *one* receptor or the presence of *several* peptide binding sites with different peptide affinities. In this regard Lee et al. (*Biophys. J. 61*, A379, 1992, abstract) have reported two important findings: (a) the N-terminal domain of BP has a propensity for helix formation, and there is interconversion between random coil and α-helix states of BP; and (b) replacement of glycines by valines enhances helix formation. These observations clearly demonstrate the existence of more than one structure for the BP in solution. In agreement with this conclusion is the fact that k_{on} for the BP blockade reaction in *Shaker* B K^+ channels has a very large Q_{10} (Murrell-Lagnado & Aldrich, 1993b); *i.e.*, temperature appears to stabilize those BP structures that are more complemental with the BP receptor. Since the presence of valines enhances helix formation and we found that the A2VA3VA5V peptide binds much tighter to the channel than the wild type peptide, it is tempting to suggest that the helical

form is preferred by the receptor over the random coil structure. On this basis a more reasonable kinetic scheme than R-1 would be

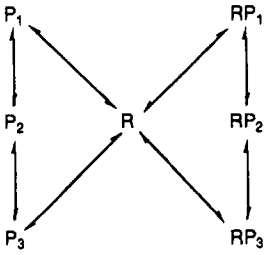

(R-2)

where P_i and RP_i (i = 1, 2, 3) are the unbound and bound forms of the different peptide conformations, respectively, and R is the peptide receptor. Each of the RP_i's gives rise to the kinetically distinguishable blocked states observed experimentally. In reaction scheme R-2 we assumed that the receptor can only bind one peptide molecule at any given time and hence the reaction is always bimolecular. On the other hand, one can imagine a bimolecular reaction as composed of two sequential steps: first, an encounter complex is formed (diffusional step), and second, the actual bound state (the peptide-bound channel complex) is produced (nondiffusional step) [*e.g.*, Schurr (1970) and Shoup and Szabo (1982)]. In this approach both the association and dissociation rate constants contain diffusion steps, and it is expected that both rates should be affected by electrostatic potential in general, and in the diffusion-controlled regime in particular [see eqs 8 and 9 in Shoup and Szabo (1982)]. We found (Figure 4B) that the effect of ionic strength on the blocking potency of the E12KD13K peptide is mainly a k_{on} affair, and therefore, it is likely that the reaction between channel and peptide is not diffusion limited. The rate-limiting step in this case would be in the nondiffusional step. It is interesting to note that the binding of E12KD13K peptide to non-inactivating *Shaker* B K^+ channels is also affected by ionic strength (Murrell-Lagnado & Aldrich, 1993a).

One of the aims of our previous study was to see whether the receptor of BP has been conserved through evolution of K^+ channels in general, and of K_{Ca} channels in particular. The BP interacts with distant K^+ channels, including K_{Ca} channels, *Shaker* B K^+ channels, and a K^+ channel from epithelial cells (Zagotta et al., 1990; Dubinsky et al., 1992; Foster et al., 1992; Toro et al., 1992; Pérez et al., 1994), but not with K_{ATP} channels (Beirao et al., 1994). In all cases, BP interacts with the internal mouth of the channels occluding ion flow (Demo & Yellen, 1991; Foster et al., 1992; Toro et al., 1992; Mayorga-Wark et al., 1993); in addition, as mentioned earlier, the BP structural characteristics that define its interaction with its receptor are the same in K_{Ca} channels (this work) and in *Shaker* B K^+ channels (Murrell-Lagnado & Aldrich, 1993a,b). Taken together, these features strongly suggest that the BP receptor of K_{Ca} channels and *Shaker* B K^+ channels are structurally homologous. In this regard, residues in the S4–S5 linker (H4) implicated in conforming the BP receptor in *Shaker* B K^+ channels (Isacoff et al., 1991) are conserved in the H4 linkers of *slo* (Adelman et al., 1992) and *mslo* (Butler et al., 1993) K_{Ca} channels with the exception of a negatively charged glutamate (E395 in *Shaker* B), indicating that the BP receptor has been conserved to a large extent through evolution of K^+ channels. Because the affinity and rate of association of the BP mutants are increased by increasing peptide net charge or decreasing ionic strength [Figures 2 and 4; see also Murrell-Lagnado and Aldrich (1993a,b)], it is likely that the BP receptor in K_{Ca} channels comprises or is adjacent to negative charges as the putative BP receptor for *Shaker* B K^+ channels (Isacoff et al., 1991). If the H4 linker of K_{Ca} channels forms part of the BP receptor is an open question.

In the Na^+ channel, the linker between domains III and IV (LIII/IV) plays a fundamental role in the fast inactivation process. Antibodies directed against or "cuts" to this protein segment greatly slowed down inactivation (Vassilev et al., 1988; Stuhmer et al., 1989). The LIII/IV contains 12 positively charged residues, which, differing from fast inactivation in *Shaker* B K^+ channels, appear not to be critical for fast inactivation in Na^+ channels (Patton et al., 1992). However, a cluster of three hydrophobic amino acids (IFM) is essential for fast inactivation (West et al., 1992), strongly suggesting that hydrophobic interactions play a crucial role in determining the interaction between the inactivating gate and its receptor. Thus, it is probable that the same structural determinants are important in K^+ and Na^+ channel inactivation, with the proviso that the internal mouth of rat brain Na^+ channels is neutral or has a very low negative charge density. In fact, the LIII/IV has been attached to the amino terminus of a non-inactivating K^+ channel, transferring to the latter the fast inactivating properties of *Shaker* A-type K^+ channels. Moreover, the same mutations that profoundly alter fast inactivation in Na^+ channels eliminated or slowed down inactivation in the chimera (Patton et al., 1993).

One surprising finding was that the voltage dependence of BP blockade was independent of the peptide net charge. This observation rules out the classical explanation of a charged blocker that moves in the electric field to reach the receptor site. An alternative explanation is that put forward by MacKinnon and Miller (1988) to explain the voltage dependence of charybdotoxin blockade of a skeletal muscle K_{Ca} channel. In this case the "voltage dependence" arises as a consequence of the efflux of K^+ when the membrane is depolarized. Positive voltages increase the degree of occupancy of a K^+ site located near the external mouth that electrostatically repels charybdotoxin from its docking position. In other words, there is not an intrinsic voltage dependence of the toxin blockade. In the case of BP we are forced to discard this possibility since we found that replacement of external K^+ by an impermeant cation does not greatly modify the voltage dependence of BP blockade. In fact, $A = 0.66$ in symmetrical 250 mM KCl (Toro et al., 1992) and $A = 0.44$ when the external KCl is replaced by an equimolar amount of NaCl (Table 1). The characteristics of the voltage dependence of BP blockade of K_{Ca} channels resemble that found for the blockade induced by saxitoxin and analogues in the batrachotoxin-activated Na^+ channel [*e.g.*, Moczydlowski et al. (1984)]. For this case, it was postulated that the receptor can exist in a low- and a high-binding affinity configuration and that the transition between these two configurations of the receptor was voltage dependent. For BP, scheme R-2 provides an economical explanation for the voltage dependence if one assumes that one or several of the interconversions between the different peptide-bound (blocked) states are voltage dependent.

ACKNOWLEDGMENT

We thank Dr. R. W. Aldrich for kindly sharing important manuscripts before publication. We also wish to thak Mr. Garland Cantrell for building the bilayer amplifier.

REFERENCES

Adelman, J. P., Shen, K.-Z., Kavanaugh, M. P., Warren, R. A., Wu, Y.-N., Lagrutta, A., Bond, C. T., & North, R. A. (1992)

Neuron 9, 209–216.
Alvarez, O., Brodwick, M., Latorre, R., McLaughlin, A., McLaughlin, S., & Szabo, G. (1983) *Biophys. J. 44*, 333–342.
Armstrong, C., & Bezanilla, F. (1977) *J. Gen. Physiol. 70*, 567–590.
Beirao, P. S. L., Davies, N. W., & Stanfield, P. R. (1994) *J. Physiol. 474*, 269–274.
Butler, A., Tsunoda, S., McCobb, D. P., Wei, A., & Salkoff, L. (1993) *Science 261*, 221–224.
Cantor, C. R., & Schimel, P. R. (1980) *Biophysical Chemistry. Part I: The conformation of macromolecules*, W. H. Freeman, San Franciso (49 pp).
Choi, K. L., Aldrich, R. W., & Yellen, G. (1991) *Proc. Natl. Acad. Sci. U.S.A. 88*, 5092–5095.
Demo, S. D., & Yellen, G. (1991) *Neuron 7*, 743–753.
Dubinsky, W. P., Mayorga-Wark, O., & Shultz, S. G. (1992) *Proc. Natl. Acad. Sci. U.S.A. 89*, 1770–1774.
Foster, Ch. D., Chung, S., Zagotta, W. N., Aldrich, R. W., & Levitan, I. B. (1992) *Neuron 9*, 229–236.
Hoshi, T., Zagotta, N., & Aldrich, R. W. (1990) *Science 280*, 533–538.
Isacoff, E. Y., Jan, Y. N., & Jan, L. Y. (1991) *Nature 353*, 86–90.
MacKinnon, R., & Miller, C. (1988) *J. Gen. Physiol. 91*, 335–349.
MacKinnon, R., Aldrich, R. W., & Lee, A. W. (1993) *Science 263*, 757–759.
Mayorga-Wark, O., Constantin, J., Dubinsky, W. P., & Schultz, S. G. (1993) *Am. J. Physiol. 265*, C541–C547.
Moczydlowski, E., Hall, S., Garber, S. S., Strichartz, G. S., & Miller, C. (1984) *J. Gen. Physiol. 84*, 687–704.
Moczydlowski, E., Uehara, A., & Hall, S. (1986) in *Ion channel reconstitution* (Miller, C., Ed.) pp 405–428, Plenum Press, New York.
Murrell-Lagnado, R. U., & Aldrich, R. W. (1993a) *J. Gen. Physiol. 102*, 949–975.
Murrell-Lagnado, R. U., & Aldrich, R. W. (1993b) *J. Gen. Physiol. 102*, 977–1003.
Nozaki, Y., & Tanford, C. (1971) *J. Biol. Chem. 246*, 2211–2217.
Patton, D. E., West, J. W., Catterall, W. A., & Goldin, A. L. (1992) *Proc. Natl. Acad. Sci. U.S.A. 89*, 10905–10909.
Patton, D. E., West, J. W., Catterall, W. A., & Goldin, A. L. (1993) *Neuron 11*, 967–974.
Pérez, G., Lagrutta, A., Adelman, J. P., & Toro, L. (1994) *Biophys. J. 66*, 1022–1027.
Schurr, J. M. (1970) *Biophys. J. 106*, 700–716.
Shoup, D., & Szabo, A. (1980) *Biophys. J. 40*, 33–39.
Solaro, C. R., & Lingle, C. J. (1992) *Science 257*, 1694–1698.
Stuhmer, W., Conti, F., Suzuki, H., Wang, X. D., Noda, M., Yahagi, N., Kubo, H., & Numa, S. (1989) *Nature 339*, 597–603.
Tanford, C. (1980) *The hydrophobic effect*, John Wiley & Sons, New York (200 pp).
Toro, L., Vaca, L., & Stefani, E. (1991) *Am. J. Physiol. 260*, H1779–H1789.
Toro, L., Stefani, E., Latorre, R. (1992) *Neuron 9*, 237–245.
Vassilev, P. M., Scheuer, T., & Catterall, W. A. (1988) *Science 241*, 1658–1661.
Villarroel, A. (1989) Mechanism of ion conduction in the large calcium-activated potassium channel, Ph.D. Dissertation, University of California, Los Angeles, CA (133 pp).
West, J. W., Patton, D. E., Scheuer, T., Wang, Y., Goldin, A. L., & Catterall, W. A. (1992) *Proc. Natl. Acad. Sci. U.S.A. 89*, 10910–10914.
Zagotta, W. N., Hoshi, T., & Aldrich, R. W. (1990) *Science 250*, 568–571.